

MIXING OF LIQUID CRYOGENS IN THE SIMULATION OF LIQUID HYDROGEN/LIQUID OXYGEN EXPLOSION HAZARDS

T.S. Luchik, K.M. Aaron, E.Y. Kwack, P. Shakkottai and L.H. Back

Jet Propulsion Laboratory
California Institute of Technology
Pasadena, California USA

ABSTRACT

Experiments simulating mixing of liquid oxygen (LO_2) and liquid hydrogen (LH_2) have been performed. The non-reactive mixtures were obtained by injecting jets of the oxidizer into a pool of the fuel simulant. Three fluid combinations were tested: LO_2 into liquid helium (LHe), liquid nitrogen (LN_2) into LHe and LN_2 into LH_2 . Experimental observations included flash X-ray and high speed video imaging, hot film anemometry, and thermocouple and diode thermometry. Results showed that the jet fluid stays coherent throughout the mixing process and that peak boiling of the pool fluid occurs shortly after jet impingement. Estimates of bulk density indicate a smaller range of variation than is currently being used for explosive yield calculations.

1. INTRODUCTION

Several of the planetary missions at the Jet Propulsion Laboratory (JPL) use Radioisotope Thermoelectric Generators (RTGs) as part of the spacecraft's power system. In carrying out the required RTG hazard definition analysis for these missions, it became evident that the potential threat to the RTGs from an explosion of liquid oxygen (LO_2) and liquid hydrogen (LH_2) as a result of a launch vehicle accident is not well defined or understood. LH_2 and LO_2 are the propellants for the National Space Transportation System (STS) (used to launch the Galileo mission and planned for the Ulysses mission) and the Centaur G' upper stage booster (planned to be used with a Titan IV and used to launch the Mariner Mark II series spacecraft). The lack of understanding stems from an inadequate data base on close-in blast characteristics for LO_2/LH_2 explosions. The existing data base, obtained during the PYRO [1] tests in the 1960's, emphasized far field blast characteristics for the purpose of determining the minimum safe distance for locating ground structures. However, it is the near field blast environment which impacts RTG safety. A survey of the available literature on LO_2/LH_2 explosions reveals inadequacies in the following areas:

1. The fluid mixing dynamics of LO_2/LH_2 prior to detonation and particularly interphase mixing, are not well understood.

Approved for public release, Distribution unlimited

Report Documentation Page				Form Approved OMB No. 0704-0188	
Public reporting burden for the collection of information is estimated to average 1 hour per response, including the time for reviewing instructions, searching existing data sources, gathering and maintaining the data needed, and completing and reviewing the collection of information. Send comments regarding this burden estimate or any other aspect of this collection of information, including suggestions for reducing this burden, to Washington Headquarters Services, Directorate for Information Operations and Reports, 1215 Jefferson Davis Highway, Suite 1204, Arlington VA 22202-4302. Respondents should be aware that notwithstanding any other provision of law, no person shall be subject to a penalty for failing to comply with a collection of information if it does not display a currently valid OMB control number.					
1. REPORT DATE AUG 1990		2. REPORT TYPE		3. DATES COVERED 00-00-1990 to 00-00-1990	
4. TITLE AND SUBTITLE Mixing of Liquid Cryogens in the Simulation of Liquid Hydrogen/Liquid Oxygen Explosion Hazards				5a. CONTRACT NUMBER	
				5b. GRANT NUMBER	
				5c. PROGRAM ELEMENT NUMBER	
6. AUTHOR(S)				5d. PROJECT NUMBER	
				5e. TASK NUMBER	
				5f. WORK UNIT NUMBER	
7. PERFORMING ORGANIZATION NAME(S) AND ADDRESS(ES) California Institute of Technology, Jet Propulsion Laboratory, 4800 Oak Grove Drive, Pasadena, CA, 91125				8. PERFORMING ORGANIZATION REPORT NUMBER	
9. SPONSORING/MONITORING AGENCY NAME(S) AND ADDRESS(ES)				10. SPONSOR/MONITOR'S ACRONYM(S)	
				11. SPONSOR/MONITOR'S REPORT NUMBER(S)	
12. DISTRIBUTION/AVAILABILITY STATEMENT Approved for public release; distribution unlimited					
13. SUPPLEMENTARY NOTES See also ADA235006, Volume 2. Minutes of the Explosives Safety Seminar (24th) Held in St. Louis, MO on 28-30 August 1990.					
14. ABSTRACT see report					
15. SUBJECT TERMS					
16. SECURITY CLASSIFICATION OF:			17. LIMITATION OF ABSTRACT Same as Report (SAR)	18. NUMBER OF PAGES 25	19a. NAME OF RESPONSIBLE PERSON
a. REPORT unclassified	b. ABSTRACT unclassified	c. THIS PAGE unclassified			

2. The detonation and/or deflagration behavior of a LO_2/LH_2 mixture, even with prior knowledge of the mixture composition, cannot be described accurately.
3. The effects of short-time scale unreacted propellants on the long time scale blast yield are not characterized. This is particularly important relative to predicting close-in blast-loading effects that accelerate debris as projectiles.

An Explosion Hazards Program [2] was initiated to address the aforementioned inadequacies with special reference to accidental LO_2/LH_2 explosions resulting from a launch vehicle accident. The program has been divided into three tasks, each focused on a separate aspect of the explosion hazard problem. Task 1 is focused on the study of the fluid dynamics and heat transfer associated with the mixing of LO_2 and LH_2 prior to explosion. Task 2 was designed to study the detonation characteristics of well defined, homogeneous mixtures of oxygen and hydrogen. Task 3 involves the study of LO_2/LH_2 detonation characteristics in a variety of simulated accidental mixing configurations. Task 3 is currently in the planning stage. This paper reports in detail on Task 1 and gives a brief description of one phase of Task 3 which is designed to link Task 1 experiments to the Task 3 experiments.

From an explosion hazards perspective, it is the initial mixing of the LO_2 and LH_2 which is of primary importance. It is believed that during the initial mixing that a detonable mixture of multi-phase oxygen and hydrogen is formed. Current predictive techniques assume that the initial blast yield is directly proportional to the bulk-mean density of the mixture. This property, bulk density, is somewhat ad-hoc since hydrogen and oxygen are immiscible. Nonetheless, it is clear to see that reasonable limits must be placed on this parameter if a predictive code is to be used to obtain realistic estimates of blast yield from full scale simulations.

The study of this problem, even in inert mixtures, presents several difficulties. The mixture is at cryogenic temperatures, it is multi-phase, multi-constituent and is transient in both energy and momentum. The oxidizer is cooled and eventually freezes while the fuel evaporates and is heated. The net result is a harsh environment to make any type of measurements.

Because it was desired to study the mixing of the fuel and oxidizer prior to detonation, simulants for either the fuel or oxidizer were used in all Task 1 tests. Initially tests were performed with LHe as the fuel simulant so that either LN_2 or LO_2 could be used as the oxidizer. This allowed a direct comparison of LN_2 to the real oxidizer, LO_2 . Later tests were performed using LH_2 as the fuel. However, only LN_2 could be used as the oxidizer simulant in this case. Thus, performing similar tests with these three inert combinations, allows one to draw conclusions on the mixing of the actual fuel and oxidizer prior to detonation.

Several scenarios were considered in the Task 1 investigation. Figure 1 shows schematically the three most credible scenarios and how each was modelled for laboratory study. The first of these, the deep mixing scenario, is reported on in this paper. These experiments

involve the mixing of two cryogenic fluids. A jet of one fluid is injected into a deep pool of a second fluid in a manner similar to that of the work of Bishop et al. [3]. Their tests showed that significant jet penetration occurred only when the more dense fluid (oxidizer simulant) was injected into a pool of the less dense fluid (fuel simulant). When the jet and host fluids were switched very little penetration and mixing occurred. Therefore in the present study, only the mixing of oxidizer simulants injected into pools of fuel simulants are considered.

Specifically reported herein is the current status of the Task 1 experimentation. Section 2 briefly describes the experimental facility, and also contains a summary of the instrumentation used in the experiments. Results of the deep pool mixing tests are presented in Section 3, and Section 4 gives the relevant conclusions on the current work and a brief discussion on planned future experimentation in this ongoing work.

2. APPARATUS

This section gives a brief overview of the facility, instrumentation and procedures used in the Task 1 experiments. For more detailed descriptions see Luchik et al. [4,5].

2.1 Facility

A schematic of the facility is shown in Figure 2. The facility consists of a primary enclosure, a secondary enclosure and three flow systems: 1) a liquid fuel transfer system, 2) a liquid oxidizer (jet fluid) transfer system and an inert gas purge system.

The primary enclosure is mainly an exhaust duct for the liquid fuel (or simulant fuel) that is boiled off during an experiment. This enclosure houses all plumbing to the oxidizer tank as well as instrumentation used for thermal and velocity measurements made during an experiment. The stainless steel dump tank used in the experiments is 14.6 cm in diameter and has a capacity of 10.4 liters. Flow out of the dump tank was controlled using a pneumatically operated-cryogenic ball valve. Because of the nature of the experiments, knowledge of the valve timing was critical and hence, the valve was calibrated. Results of the calibrations showed that the valve, when operated at 100 psi, responded to the operator in 60 ms and went from the fully closed position to the fully open position in 40 ms. These values were independent of the overall time that the valve was open. The valve response is shown in Figure 3. The flow rate out of the dump tank was controlled by regulating the pressure of the fluid inside the tank. An interface at the bottom of the enclosure is used to seal the Pyrex glass experimental dewar to the enclosure. The dewar has a diameter of 14.3 cm and is roughly one meter in length. Pyrex glass was used to enable visual observation of the experiments. Located at the top of the primary enclosure, was a 10.2 cm diameter exhaust stack where the fuel evaporation rate was measured. The exhaust gas then flowed into a dilution duct where the exhausted fuel was diluted below its flammability limit and was exhausted to the atmosphere. A schematic of the primary enclosure, dump tank, experimental dewar and instrumentation is shown in Figure 4.

As shown in Figure 2, the primary enclosure was located inside the secondary enclosure. This enclosure was purged free of oxygen prior to each experiment and the oxygen level was monitored throughout the experiments using a Teledyne Analytical Systems Model 8000 gas detection system. Purging served two purposes. First, removing all of the air (oxygen) excludes the possibility of an accidental explosion during an experiment. Second, removing all of the oxygen from the environment and replacing it with nitrogen greatly enhanced the visual observation of the experiment, since no water vapor was available in the environment to condense on the outside of the experimental dewar. This purging of the secondary enclosure and diluting of the fuel exhaust was accomplished using an inert gas purge system [4].

2.2 Instrumentation

Chromel-constantan thermocouples (type E) were chosen for these experiments based on arguments presented by Barron [6] and ASTM [7]. However, as noted by Barron, no commercial thermocouple is useful below 30-40K because of the lack of sensitivity at these low temperatures. Because the experiments performed are transient in nature, the temporal response of the instrumentation is quite important. The size of the thermocouples chosen for the experiments was 76 μm which had a response of about 8 ms (90%). This size was a good compromise between speed and robustness (the experiments were fairly violent and smaller thermocouples did not survive the environment with regularity).

Cryodiodes were used in locations where sub-40K temperatures were expected. The sensitivity of a cryodiode is excellent at low temperatures. However, the cryodiode does have two major disadvantages. The diodes have response times which varied with the ΔT due to the large thermal capacitance of the can housing the diode. Times as great as 2 seconds were measured for a ΔT of 200K. Although the diodes were quite robust themselves, the wiring to the diode was delicate and often broke during experimentation.

Pressures in the primary and secondary enclosures and in the dump tank were measured using Validyne pressure transducers. The transducers are fairly standard strain gage type transducers. Temperature effects at the transducer were minimized by using a length of Tygon tube from the point of measurement to the transducer, which was maintained nominally at 300K.

Hot film anemometers and a pitot-static probe were used to measure velocities of the fuel boil-off gas at the mouth of the experimental dewar while only a hot film anemometer was located in the stack of the primary enclosure. However because of difficulties when helium was used as the fuel simulant, only the stack anemometer yielded useful quantitative information.

The hot-films had better accuracy and time response than the pitot probe. However, the hot-films were far more difficult to calibrate since they had to be calibrated over a range of temperatures and velocities. A typical calibration equation is given by equations (1) and (2).

$$u = (-0.753 + 13.6 E_{\text{mod}}^2)^{2.5} \quad (1)$$

where

$$E_{\text{mod}} = \frac{E_{\text{hf}}}{(T_w - T_g)^{0.45}} \quad (2)$$

and T_w is the hot film temperature, E_{hf} is the anemometer output in volts, T_g is the gas temperature in K, and u is velocity in m/s. From this equation it is clear to see that the accuracy of the velocity measurement is largely dependant on the voltage output of the anemometer and the measurement of gas temperature in the vicinity of the probe. Both of the values vary with time during an experiment. A partial calibration curve corresponding to the above equations is shown in Figure 5. Details of the hot film calibrations are give by Kwack et al. [8]. The pitot-static probe measures velocity using Bernoulli's equation

$$u = (2\Delta P / \rho_g)^{0.5} \quad (3)$$

and

$$\Delta P = \text{constant} * E_{\text{pitot}} \quad (4)$$

Here ΔP is the pitot-static pressure difference, ρ_g is the gas density and E_{pitot} is the pressure transducer output. Although the equation for the pitot probe looks simpler than the hot film calibration equation, note that the density of the gas is a function of temperature. Thus, the experimental measurement is not simpler than for the hot-film, only the calibration is simpler.

Measurements at the exhaust stack were simpler than those at the mouth in that the environment was less harsh than that at the mouth. The temperature of the gas at this location varied from 50 K to about 250K. Thus, a large range of calibration was necessary. At the mouth of the dewar, the temperature varied little, but the temperature at this location was seldom greater than 25K during the experiment. The cold temperatures tended to destroy hot films after repeated cycling.

A Spin Physics model SP-2000 high speed motion analyzer was used to obtain video recordings of each experiment. For these experiments, recordings were obtained in excess of 500 fps. Typically, the vertical field of view was 45 cm with a minimum spatial resolution of 2.2 mm by 2.2 mm. The experiment was back lighted with 3 quartz halogen lights which yielded good contrast between the host and jet fluids. The video images were digitized and some image processing techniques were applied to the images to help better define the mixing zone at selected times during the experiments. However, the image processing techniques did not yield any additional information that had not already been gathered from simple viewing of the video tapes.

A Hewlett-Packard 300 kV flash X-ray system was used to obtain an X-ray of the mixing process. This yielded one observation per experiment with a 50 ns exposure. Each head

has a beryllium window, rather than aluminum, to allow better transmission of the low energy X-rays, which are more sensitive to low molecular weight matter, like LN_2 , LO_2 , LH_2 and LHe . A wide variety of X-ray receivers have been used in this system including a Science Applications Incorporated RTR 300 X-ray image intensifier, DuPont medical and non-destructive testing (NDT) films, screens and cassettes, and Eastman Kodak films. A large number of tests were run using various combinations of the above products as well as varying the source to object distance and flash X-ray output voltage. The "best" receiver tested was the combination of three Dupont products: a Dupont Kevlar Cassette with Chronex Quanta Fast Detail screens and either NDT 57 or Chronex 4 film. However, even with this combination, no quantitative results have been obtained with the X-ray system to date. The reason for this is that there exists a lack of contrast between the jet and host fluids used in these experiments.

Although the X-ray images have not given quantitative information, they have yielded valuable information which has been used in developing a qualitative model of the initial mixing during the mixing of the jet and host fluid. It should be noted that the only imaging technique, other than neutron absorption, able to penetrate the mixing zone is the flash X-ray technique.

A schematic of the data acquisition system is shown in Figure 6. The host computer is an IBM PC compatible. The main function of the compatible during data acquisition is as a memory device for the high speed A/D boards. Data sampling occurred over 23 channels at a rate of 100 scans per second. As can be seen from the figure, the hot wire/film, cryodiode and pressure transducer data are fed directly into the A/D boards while the thermocouple information must be passed through an intermediate amplifier. The A/D board also signals the host computer at appropriate times to trigger the dump tank operator valve and the flash X-ray system. The host achieves the triggering process through the use of a parallel I/O board and relay board. The host computer also controls the Spin Physics motion analyzer through an RS-232 port.

3. RESULTS

The independent variables for the experiments were the jet velocity, the jet momentum, the dump duration, and the distance between the nozzle exit plane and the free surface of the pool fluid. This distance is referred to as ullage herein. For the various experiments all of the independent variables were varied.

Initially, liquid helium was used as a fuel simulant for the purpose of comparing liquid nitrogen to liquid oxygen. This would prove useful in interpreting the liquid hydrogen/liquid nitrogen experiments. Physical properties of all of the fluids used in the experiments are listed in Table 1. More information on cryogenic fluid properties can be found in Barron [6], Sychev et al. [9,10,11] and Scott [12]. From this table, to a first order approximation, LN_2 appears to be a good simulant for LO_2 in that the thermophysical properties of the fluids are similar. Helium, on the other hand, has one significant property difference from hydrogen, the latent heat of vaporization. This value for helium is approximately a factor of 20 lower for helium than that for hydrogen. Since this property

directly affects boiling, the helium evaporation rate cannot be used in any way to approximate hydrogen evaporation. Also, because of the relatively low latent heat of vaporization of liquid helium (21 kJ/kg), the parasitic boil off of helium was high, making the ullage very difficult to control with good accuracy.

Varying the nozzle diameter was one way of controlling the mass flow rate of the jet independent of the jet velocity. However the jet diameter played another important role in the experiment. From an X-ray perspective, it was preferable for the jet to be as large in diameter as possible to maximize X-ray contrast between the jet and the host fluid. Fluid dynamically, a small diameter jet is preferable to minimize wall effects. These, of course, are conflicting requirements. Nozzles with diameters of 3.17 mm, 6.34 mm and 12.7 mm were used in the experiments, but only experiments with the 12.7 mm diameter nozzle yielded useable X-radiographs.

Table 1. Some properties of helium, hydrogen, nitrogen and oxygen.

	Helium	Hydrogen	Nitrogen	Oxygen
T_{BP} (K) (1 atm)	4.2	20.26	77.35	90.18
T_{FP} (K) (1 atm)	-----	13.8	63.15	54.36
ρ_{BP} (kg/m ³)	125	70	807	1141
ρ_{BP} (kg/m ³)	17	1.3	4.6	4.5
h_{fg} (kJ/kg)	21	454	199	213
h_{fs} (kJ/kg)	-----	-----	25.1	13.8
$h_{\gamma-\beta}$ (kJ/kg)	-----	-----	-----	23.4
$T_{\gamma-\beta}$ (K)	-----	-----	-----	43.8
$h_{\beta-\alpha}$ (kJ/kg)	-----	-----	~8.4	2.9
$T_{\beta-\alpha}$ (K)	-----	-----	35.6	23.6
c_p (kJ/kg-K)	5.40	12.15	4.73	1.0
$c_{p_{gBP}}$ (kJ/kg-K)	4.98	9.66	2.13	1.67
$c_{p_{IBP}}$ (kJ/kg-K)	-----	-----	1.88	1.42
$c_{p_{sFP}}$				

3.1 Helium Test Results

Over 70 separate helium experiments were performed where complete data sets were collected, roughly one-half with LO₂ as the jet fluid and one-half with LN₂ as the jet fluid. The velocity range from 3 m/s to 11 m/s was covered and ullage was varied from 20 cm to 76 cm. The purpose of performing tests with helium was to gain some experience in the mixing of two cryogenic fluids in a totally inert environment, but more importantly to determine the similarities and differences in LN₂ and LO₂ as jet fluids. Since later tests would only involve mixing of LN₂ with LH₂, a good working knowledge of this comparison would allow any extrapolation of the present results to the real situation where LO₂ and LH₂ would be involved.

Although many tests were run, not all tests were different. Several were similar by design to obtain information on the run to run variation of the experiments. The results of these

replicate tests were quite good. Not only was there qualitative agreement in the data but also the quantitative data agreed quite well. An example of this agreement is shown in Figure 7 for the measured helium gas mass flow rate at the stack, the parameter most sensitive to run to run variations. In this Figure, the jet velocity is 3.5 m/s, the nozzle diameter is 6.35 mm and the dump duration is 0.45 sec.

Temporal contours of the mixing zone are shown in Figure 8 for an LN_2/LHe experiment and an LO_2/LHe experiment. Each of these experiments was nominally at the same conditions, a jet velocity of 3.2 m/s, 6.35 mm nozzle and 22 cm ullage, with only the jet fluid being different. The solid contours are "mixing zone" contours at 20 msec time increments while the dashed contour at time $t = 0$ is the estimated liquid "jet" contour. This estimate of the actual jet fluid location is based on experiments with an LN_2 jet into cold helium gas ($T < 20\text{K}$) and from X-ray observations. From those experiments involving the LN_2 jet into cold He gas it was seen that a mixing zone formed between the relatively warm jet fluid and cold He gas. From this knowledge, we see that prior to impingement of the liquid jet on the helium free surface, a mixing zone is formed. This figure is another example of excellent agreement between the LN_2 and LO_2 jet studies.

It is sufficient to say that the results of the LN_2 tests and the LO_2 agreed well in almost every way with one exception. Information pertaining to the size of the frozen particles observed in the experiments differed. It was noted from the experiments that the solid particles become visually observable at the head of the jet initially and a short time later at the outer most extremity of the mixing zone generally near the region of the initial jet impingement. The particles are first seen about 200 to 400 msec after jet impingement for all tests, and this time does not vary systematically with any of the independent variables nor with the jet fluid. As observed from the motion of the particles in the case of the LN_2 jet, they are platelet in shape and fall through the liquid helium at a velocity of about 1 m/s. Quantitative information obtained, based on a sample of 500 particles, indicate that the average size of a particle is 38 mm^2 with sizes ranging from 4 mm^2 to 130 mm^2 , and in general the platelets are less than 1 mm thick. The particles in the case of the LO_2 jet were smaller than that of the LN_2 jet and were generally smaller than the resolution of the video system used. However, large particles could be visualized occasionally. Although no mean size data were obtained for O_2 , it was noted that the large O_2 particles were also platelet shaped. The size difference was the only significant difference noted between the nitrogen and the oxygen jets.

The solids seen in all of the experiments were much larger than is predicted from instability theory, which predicts droplet sizes of the order of microns. Thus, measurements of particle size would indicate that freezing is occurring at the jet outer extremity while the jet is still intact which agrees with the X-ray images that show that the jet is largely coherent during the mixing process. However, this hypothesis is impossible to verify experimentally since the mixing bubble cannot be penetrated with enough spatial resolution and dynamic range to visualize the actual solidification process. The smallest particles discernable, because of the pixel resolution of the video system, was 4 mm^2 for most of the tests, but as small as 1 mm^2 in some cases. Therefore, some small particles may be formed in the mix but are not discernible optically with the current instrumentation.

3.2 Hydrogen Test Results

For the hydrogen tests as in the helium tests, several tests at similar conditions were performed to determine the run-to-run variation of the tests. As was seen in the helium tests, the duplicate experiments yielded similar results.

Figure 9 shows some of the general mixing dynamics for the experimental configuration obtained from the hydrogen tests. The jet impinges on the host fluid which causes boiling of the host and cooling to the eventual freezing point of the jet. As the jet continues to penetrate, a mixing pocket forms which contains some mixture of the gas and liquid state of the host and liquid and solid state of the jet. As time progresses, the fluids within the mixing pocket transfer enough heat between each other so that some freezing of the jet occurs while the host continues to boil off. During the initial mixing of the jet and host fluid the mixing zone is optically too dense to penetrate using conventional optics. However, the radiographs have shown that the jet fluid essentially stays intact and has a diameter approximately equal to that when it leaves the nozzle. Figure 10 shows the mixing zone developed by a 12.7 mm jet of LO_2 with an impingement velocity of 3.2 m/s into LHe approximately 0.2 sec. after jet impingement (A radiograph of an LO_2 jet into liquid helium is shown in Figure 10 because the radiographs obtained from the hydrogen tests were just not publication quality, although they did contain the same information as the radiograph shown). The mixing zone contains both jet and host fluid in its liquid state as well as vaporized host. A comparison of visual images to the radiographs showed that the mixing zone is roughly 5 to 8 times the diameter of the jet. The X-radiographs show further that within the mixing zone the host is largely gas on a volume basis. Somewhat later in the mixing process (about 200 msec to 400 msec) solidification of the jet occurs at the head of the jet and near the point of initial impingement.

Mixing zone contours obtained from images taken with the Spin Physics motion analyzer are shown in Figure 11. These images were obtained for a 3.05 m/s jet of LN_2 into a pool of hydrogen. The nozzle diameter in this experiment was 12.7 mm. Each contour represents an instant in time and the contours are separated in time by 20 ms. As in Figure 8, the jet contour at impingement has been shown by a dashed line and was determined in a similar manner to that of Figure 8. Immediately after impingement, the jet velocity is significantly decreased from its initial velocity. The velocity is less for smaller diameter jets. Figure 12 shows the variation of an average of the jet penetration speed with nozzle size and time. A second surge generates a mixing zone that appears similar to the initial mixing zone. As with the helium studies, very little can be said on the radial rate of formation of the mixing zone other than it does develop more slowly radially than axially.

From the mixing zone impingement contours and from the Spin Physics video in general, several pieces of information were obtained. These include an estimate of the bulk or mean density within the mixing zone, and information on the solidification of the jet fluid.

One method of obtaining the bulk density within the mixing zone was obtained by assuming that the mixing zone volume can be described by a pseudo-body of revolution of a given time contour. Note that since the mixing zone contours are not symmetric, it is only

necessary to rotate each contour through 180° and disregard the surface discontinuity at 180°. Then if one assumes that all of the hydrogen within the mixing volume is in the gaseous state at its normal boiling point and all of the jet fluid is in its liquid state at the normal boiling point, the bulk density of the mixing zone can be calculated using

$$\bar{\rho} = \frac{\dot{m}_{jet}\Delta t + \rho_{GH_2} \left(V_{mix} - \frac{\dot{m}_{jet}\Delta t}{\rho_{jet}} \right)}{V_{mix}} \quad (5)$$

which can be manipulated to obtain

$$\bar{\rho} = \rho_{GH_2} + \frac{\dot{m}_{jet}\Delta t}{V_{mix}} \left(1 - \frac{\rho_{GH_2}}{\rho_{jet}} \right) \quad (6)$$

Here \dot{m}_{jet} is the mass flow rate of jet into the mixing zone and V_{mix} is the volume of the mixing zone at Δt seconds after impingement. This is an upper estimate since all of the jet fluid is assumed to be participating in the heat transfer involved in boiling the host fluid. Table 2 shows the average values of the upper estimate of bulk density within the mixing zone at early times after impingement obtained from the various experiments. All averages were obtained from mixing zone contours 120 msec after impingement of the jet. For comparison the density of hydrogen vapor at 20.3K is 0.0013 g/cm³. The estimated values for an oxygen jet were made simply by assuming that the volume occupied by the LN₂ had the density of LO₂ at its normal boiling point. These results are consistent with what was experimentally found in the helium tests.

This estimated bulk density does vary with the radius of the jet, a result seen in the helium tests. As is shown in Luchik et al. [5], a simple argument can show this to be the expected case which yields

$$\frac{\bar{\rho} - \rho_{GH_2}}{\rho_{jet} - \rho_{GH_2}} \propto \frac{u_{jet}\Delta t}{\ell} \frac{r_{jet}^2}{r_{jet}} \approx C_1 r_{jet} \quad (7)$$

A second method, which estimates the minimum bulk density can be made from knowledge that the jet largely remains intact in the mixing zone. This indicates that only a portion of the original jet fluid is taking part in the heat transfer required to boil the hydrogen. The analysis is identical to that in Luchik et al. [5] except that H₂ has been substituted for He. The result is the following equation:

$$\bar{\rho}_{min} = \rho_{GH_2} \left(1 + \frac{h_{fg,H_2}}{\Delta h_{jet,max}} \right) \quad (8)$$

The maximum enthalpy change in the jet fluid is achieved by cooling it to the liquid pool temperature (20.3K for liquid hydrogen). $\Delta h_{jet,max}$ has the value of 124 kJ/kg for N₂ and 136 kJ/kg for O₂. Doing this assumes that the minimum jet mass is involved in the heat

transfer required for boiling heat transfer, thus yielding the minimum bulk density. Substituting the values for the thermophysical properties gives $\bar{\rho}_{\min} = 0.0059 \text{ g/cm}^3$ for LN_2 jets and $\bar{\rho}_{\min} = 0.0055 \text{ g/cm}^3$ for LO_2 jets. These values are roughly a factor of two lower than the upper estimate values obtained for the 3.17 cm diameter nozzle indicating that even with that small nozzle size only about one-half of the jet was participating in the heat transfer to the hydrogen. These results are significant in that current predictive techniques cover a range of bulk densities with an upper limit more than one order of magnitude greater than the maximum values presented here.

Table 2. Bulk density estimates during initial jet impingement.

Jet Velocity (m/s)	Nozzle Dia. (mm)	LN_2 jet $\bar{\rho}$ (g/cm ³)	LO_2 jet $\bar{\rho}$ (estimated) (g/cm ³)
3.0-5.0	3.17	0.013	0.015
3.0-5.0	6.35	0.014 ± 0.006	0.018
3.0-5.0	12.7	0.023 ± 0.009	0.032

The size of most of the solid particles in these experiments varied from 7 mm² to 70 mm² with the largest particle seen being 350 mm². The particles in the hydrogen tests appeared platelet in shape. The size information for the N_2 particles as well as the shape is consistent with what had been seen in the helium tests with a LN_2 jet. The particle size was observed to increase as the jet diameter was increased. Particle information for N_2 was found to be independent of the pool fluid with which it was mixed. This leads to the conclusion that SO_2 particles generated in a mix of LO_2/LH_2 would be similar to those in the LO_2/LHe tests.

The instantaneous temperature of the H_2 gas at the mouth of the dewar is given in Figure 13 while the instantaneous evaporation rate of H_2 is presented in Figure 14. Results from three different experiments are shown to show the consistency from experiment-to-experiment. Nominal conditions for these experiments are a 12.7 mm diameter jet of N_2 flowing with jet velocity of 3.5 m/s for a period of 0.65 sec. In all cases the ullage was roughly 42 cm. Note that impingement of the jet occurs about 0.24 seconds after the dump valve has been energized ($t = 0$) and that the gas temperature prior to mixing is 70-100K due to heat transfer from the surroundings. As the rate of evaporation increases, the gas exits the dewar without exchanging heat because the gas residence time in the dewar has decreased. The "peak and valley" nature of the data shown in the graph are believed to be related to the surging of jet fluid in the mixing region seen in the video images. Although not shown, the time at which peak boil off occurred did not vary appreciably. The value of peak boil off was found to vary with the nozzle diameter for a given jet velocity. This result suggests that a principle parameter in the early mixing is the diameter of the jet. More work is needed to verify this trend.

Integrated values of the hydrogen boiled off from a visual displacement measurement along with some representative data taken from the hot-film at the mouth of the experimental

dewar are given in Table 3. The purpose of this is to show the accuracy of the hot-film data. Individual values of the ratio of hydrogen boiled off to jet fluid added varied from 0.16 to 0.26.

Table 3. Comparison of time integrated hot film data and hydrogen boil off displacement measurement.

Run	\dot{m}_{jet} (g/s)	Δm_{jet} (g)	Δm_{LH_2} (g)	$\Delta m_{GH_2, HF}$ (g)	$\frac{\Delta m_{GH_2, HF}}{\Delta m_{jet}}$
663	306	138	23	25.1	0.18
664	306	199	40	40.8	0.21
665	306	199	37	39.6	0.20
666	306	199	44	41.9	0.21

The values obtained are reasonable and can be shown analytically by assuming that a small amount of jet fluid is dumped into a large container of LH_2 and that the final equilibrium temperature of the nitrogen in the hydrogen bath is 20.3 K, then we can develop the relationships (see Luchik et al. [5] for derivation)

$$\frac{\Delta m_{H_2}}{\Delta m_{jet}} = \frac{\Delta h_{jet, max}}{h_{lg, H_2} + c_{p, GH_2}(T_{GH_2, Final} - T_{BP, H_2})} \quad (9)$$

where c_p is the specific heat, h_{lg} is the latent heat of vaporization, T is temperature and the subscripts H_2 and jet refer to the given constituent. $\Delta h_{jet, max}$ is as before, 124 kJ/kg for N_2 and 136 kJ/kg for O_2 and represents the energy release from the jet fluid when cooled to 20.3K. Assuming that the hydrogen boils off and leaves the control volume at it's boiling point, one can obtain the maximum ratios of hydrogen boiled to jet fluid added. These values are 0.27 and 0.30 for N_2 and O_2 respectively.

However, if the hydrogen gas leaving the control volume is allowed to exchange heat with the jet fluid, the mass ratios can be less than the maximum. Since hydrogen has a high heat of vaporization (454 kJ/kg) and a relatively low specific heat the variation of boil off with gas exit temperature is small as is shown in the following equation for LN_2/LH_2 .

$$\frac{\Delta m_{H_2}}{\Delta m_{N_2}} = \frac{124.0 \text{ kJ/kg}}{12.15 \frac{\text{kJ}}{\text{kg-K}}(\Delta T_{GH_2, Final}) + 454 \frac{\text{kJ}}{\text{kg}}} \quad (11)$$

Here $\Delta T_{GH_2, Final}$ is the amount of temperature rise, above the normal boiling point, of the gaseous hydrogen exiting the control volume. A similar equation results for LO_2 with only numerator being changed to 136 kJ/kg. The boiling of hydrogen occurs at 20.3 K but the temperature that hydrogen leaves the control volume can be higher than that because of heat transfer from either the liquid jet fluid or the relatively warm solid particles to the gaseous hydrogen. Table 4 summarizes the results obtained from the above equation for

both LO₂ and LN₂. Using an average boil-off ratio of 0.2 (From Table 3), Table 4 shows that the average temperature of the hydrogen gas exiting the experimental dewar was 13K warmer than its normal boiling point. However, the thermocouple at the mouth of the dewar only indicated a superheat of about 5K during active boiling. No reason is offered for this discrepancy. This implies that between 73% and 88% of the jet fluid energy went into the actual vaporization of the hydrogen liquid pool, on average.

Table 4. Equilibrium calculation of the ratio of liquid hydrogen vaporized to liquid nitrogen or liquid oxygen solidified.

$T_{\text{GH}_2, \text{Final}} - T_{\text{BP, H}_2}$	$\Delta m_{\text{GH}_2} / \Delta m_{\text{LN}_2}$	$\Delta m_{\text{GH}_2} / \Delta m_{\text{LO}_2}$
0.0	0.27	0.30
5.0	0.24	0.26
10.0	0.22	0.24
15.0	0.19	0.21
20.0	0.18	0.20
25.0	0.16	0.18

4.0 SUMMARY AND FUTURE WORK

Deep pool mixing studies of LN₂/LHe, LO₂/LHe and LN₂/LH₂ have been completed. The present mixing studies included varying jet velocities, jet dump duration times, jet diameter and ullage spaces. However, the qualitative nature of the mixing zone does not seem to be greatly affected by these variables although the rate of formation of the mixing zone occurs more rapidly when LHe is the pool fluid than when LH₂ is the pool fluid. Ullage space seems to have little effect on the liquid-liquid mixing zone. Heat exchange between the liquid jet and the colder gas in the ullage space seems to have little effect on the dynamics of the liquid-liquid interaction

The preliminary experiments with LO₂ and LN₂ as the jet fluids showed that N₂ was an excellent simulant for O₂ in all respects except one. The one aspect where N₂ differed from O₂ was in the formation of solid particles. All of the particles observed in the experiments were similar in shape. The motion of these particles in the high-speed video recordings indicated that the particles were platelet in shape. However, in the helium studies, a large number of particles were visualized when LN₂ was the jet fluid whereas when LO₂ was the jet, far fewer particles were clearly visualized. It is believed that the O₂ particles were present, but were too small to be seen with the resolution of the camera system. The solid particles for the N₂ jet were the same size and shape regardless of the pool fluid into which the LN₂ was injected.

The axial rate of formation of the mixing zone slowed with time after impingement of the jet with the formation nearly stopping 150 to 200 ms after jet impingement. Some 50 to 150 ms passed before a second surge of jet fluid was seen. The radial rate of formation of the mixing zone was very slow. Maximum boiling of the hydrogen pool occurred 200 to 300 ms after jet impingement and the value of the maximum boil off rate scaled with the nozzle

diameter for a given jet velocity. This indicates that the maximum boil off rate was heavily dependant on the surface area of the jet (ie. the jet could be modeled as a column of fluid submerged in a pool of hydrogen). This further indicates that the amount of jet fluid sheared from the jet is small. This is further evidenced by the large discrepancies in the maximum and minimum bulk densities and the results of the flash radiographs.

Two different values were obtained for bulk density. One assumed that all of the jet fluid was involved in the heat transfer required to vaporize the hydrogen in the mixing volume. This estimate is a maximum estimate for bulk density since all other indicators show that the entire jet mass is not diffused throughout the mixing zone. The second estimate for bulk density was based on heat transfer concepts. It assumed that the minimum jet mass transferred all of the available energy to the hydrogen and that this energy was used for vaporization only. This estimate is, by definition, the minimum bulk density in the mixing zone allowed by the physics of the problem. The values determined as the upper limit on bulk density for a liquid nitrogen jet into a pool of hydrogen varied with the nozzle diameter and had values ranging from 0.013 g/cm³ for the 3.17 mm nozzle to 0.023 g/cm³ for the 12.7 mm nozzle. Values for $\bar{\rho}$ were then estimated for LO₂ jets into LH₂. These values were only slightly higher than those for LN₂. The minimum value of bulk density, as determined by analysis, for a LO₂/LH₂ mixture was $\bar{\rho}_{\min} = 0.0055$ g/cm³. This range of experimentally/analytically determined values are significantly lower than the estimates being used in predictive detonation environment techniques which use upper limit values as high as $\bar{\rho} = 0.4$ g/cm³.

The next series of experiments in Task 1 of this continuing program is a study of the "Range Destruct" mode of the Titan IV/Centaur G' configuration (see Figure 1). Here a small charge located on the side of the Centaur tanks is detonated causing an axial rip in the fuel and oxidizer tanks to occur. This takes place while the payload fairing (PLF) of the launch vehicle is still in place. Liquid fuel and oxidizer pour out of the tanks and are trapped in the PLF space. A portion of each of the propellants flash vaporize since the initial pressure in the propellant tanks is significantly higher than that in the PLF. Also, as these fluids flow out of their respective tanks, they can contact the relatively hot surface of the PLF, augmenting the vaporization of each of the fluids as well as intermix, cooling some of the oxidizer while vaporizing the fuel. Because a detonable mixture of gaseous fuel and oxidizer will essentially encompass the RTGs in the payload, knowing the gas composition in this region as a function of time is of critical importance from a safety viewpoint. A simulation of such an event is planned for the laboratory with LN₂ being substituted for the oxidizer. All of the instrumentation described in this paper will be used in that experiment as well as a novel acoustic technique for determining the gas composition at several points in the flow as a function of time.

The Task 3 work planned for the future involves actual jet mixing of LO₂ and LH₂ in a manner similar to that described in this text. If the O₂/H₂ mixture does not auto-ignite after a prescribed period, a charge will be used to initiate the O₂/H₂ reaction. During these tests both near and far field detonation wave characteristics will be measured. JPL's direct interest in this problem is the near field. In the near field, over-pressures, blast loading and fragment dynamics are of importance to the RTG safety issue and will thus be the focus

of the JPL effort. Tests are also being designed so that the contribution of the air environment to the various blast characteristics can be separated from those directly due to the propellant oxidizer.

ACKNOWLEDGEMENTS

The work described in this paper was carried out in the Applied Technologies Section of the Jet Propulsion Laboratory, California Institute of Technology, under Contract with the National Aeronautics and Space Administration. The encouragement of M.J. Cork, Launch Approval Engineering, JPL Flight Project Office, and R.M. Clayton, Task Manager of the LO₂/LH₂ Explosion Hazards Program, is gratefully acknowledged. The assistance of Gracio Fabris and Dennis O'Conner during the initial stages of experimentation, and Wayne Bixler, Stan Kikkert and Ken Harstad throughout this continuing work is also acknowledged. Finally, the authors wish to thank John Fisher of DuPont for providing X-ray films, screens and cassettes as well as his technical advice and assistance.

NOMENCLATURE

c_p	specific heat
E	output voltage
h_{fg}	heat of vaporization
h_{fs}	heat of fusion
ℓ	liquid penetration distance at time when bulk density was calculated
Δm	mass difference
\dot{m}	mass flow rate
T_g	gas temperature
T_{probe}	hot film substrate temperature
T_w	hot film/wire temperature
t_e	valve energize time
Δt	time increment
u	axial velocity
V_{mix}	mixing volume

Greek Symbols

ρ	density
$\bar{\rho}$	bulk density
τ	time constant

Subscripts

BP	boiling point
FP	freezing point

g
jet
l
s

gas value
jet
liquid
solid

REFERENCES

- [1] Willoughby, A.B., Wilton, C., & Mansfield, J. 1968, Liquid propellant explosive hazards. Final Report, AFRPL TR-68-92, URS Research Company.
- [2] Massier, P.F., Marshall, J.W., & Clayton, R.M. 1988, Liquid hydrogen/liquid oxygen explosion hazards program plan. JPL D-5113, Internal Document, Jet Propulsion Laboratory, Pasadena, CA.
- [3] Bishop, C. V., Benz, F. J., & Ullian, L. J. 1986, Mixing of cryogenic fluids and predicted detonation properties for multi-phase liquid oxygen and liquid hydrogen, Presented at the 1986 JANNAF Propulsion Meeting.
- [4] Luchik, T.S., Aaron, K.M., Fabris, G., Clayton, R.M., & Back, L.H. 1989, Cryogenic mixing processes in the simulation of LO_2/LH_2 explosion hazards: Experimental facility and initial results with LN_2/LHe . JPL D-6394, Internal Document, Jet Propulsion Laboratory, Pasadena, CA.
- [5] Luchik, T.S., Aaron, K.M., Kwack, E., Shakkottai, P., Clayton, R.M., & Back, L.H., 1990, Cryogenic mixing processes in the simulation of LO_2/LH_2 explosion hazards: Results with LN_2/LHe and LO_2/LHe . JPL D-6987, Internal Document, Jet Propulsion Laboratory, Pasadena, CA.
- [6] Barron, R. F. 1985, Cryogenic Systems, (Monographs on Cryogenics), pp. 13-58, Oxford University Press, New York.
- [7] Manual on the use of Thermocouples in Temperature Measurements, ASTM special publication 470A, 1974. American Society for Testing and Materials, Philadelphia.
- [8] Kwack, E., Shakkottai, P., Luchik, T.S., Aaron, K.A., Fabris, G., & Back, L.H. 1990, Hot-Film calibrations at cryogenic temperatures, Submitted to Experiments in Fluids.
- [9] Sychev, V.V., Vasserman, A.A., Kozlov, A.D., Spiridonov, G.A., & Tsymarny, V.A. 1987a, Thermodynamic Properties of Nitrogen, Hemisphere Publishing Corp., New York.
- [10] Sychev, V.V., Vasserman, A.A., Kozlov, A.D., Spiridonov, G.A., & Tsymarny, V.A. 1987b, Thermodynamic Properties of Oxygen, Hemisphere Publishing Corp., New York.

- [11] Sychev, V.V., Vasserman, A.A., Kozlov, A.D., Spiridonov, G.A., & Tsymarny, V.A. 1987c, Thermodynamic Properties of Helium, Hemisphere Publishing Corp., New York.
- [12] Scott, R.B. 1959, Cryogenic Engineering, D. Van Nostrand Co. Inc., Princeton, NJ.

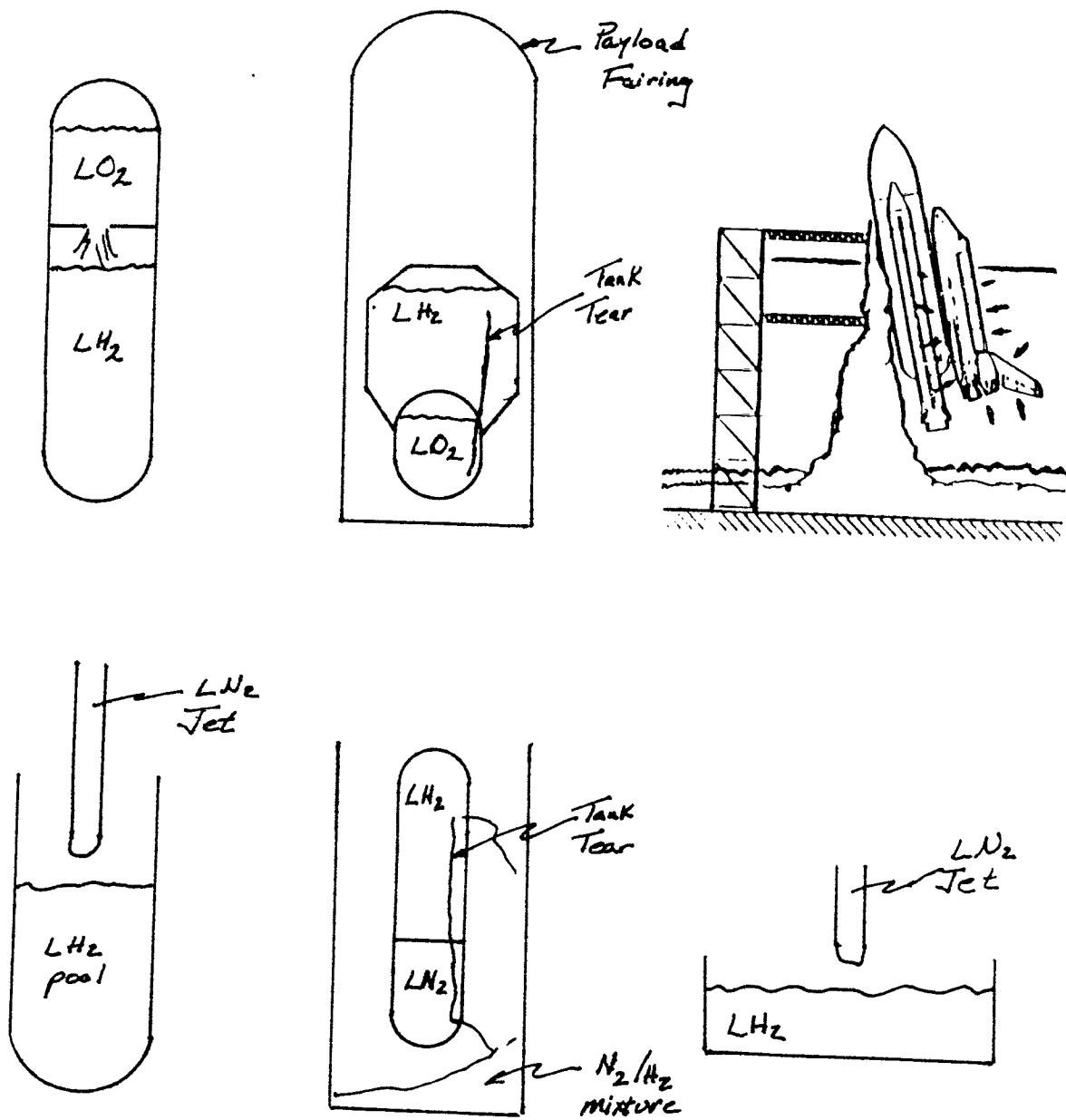


Figure 1. LO_2/LH_2 accident mixing scenarios.

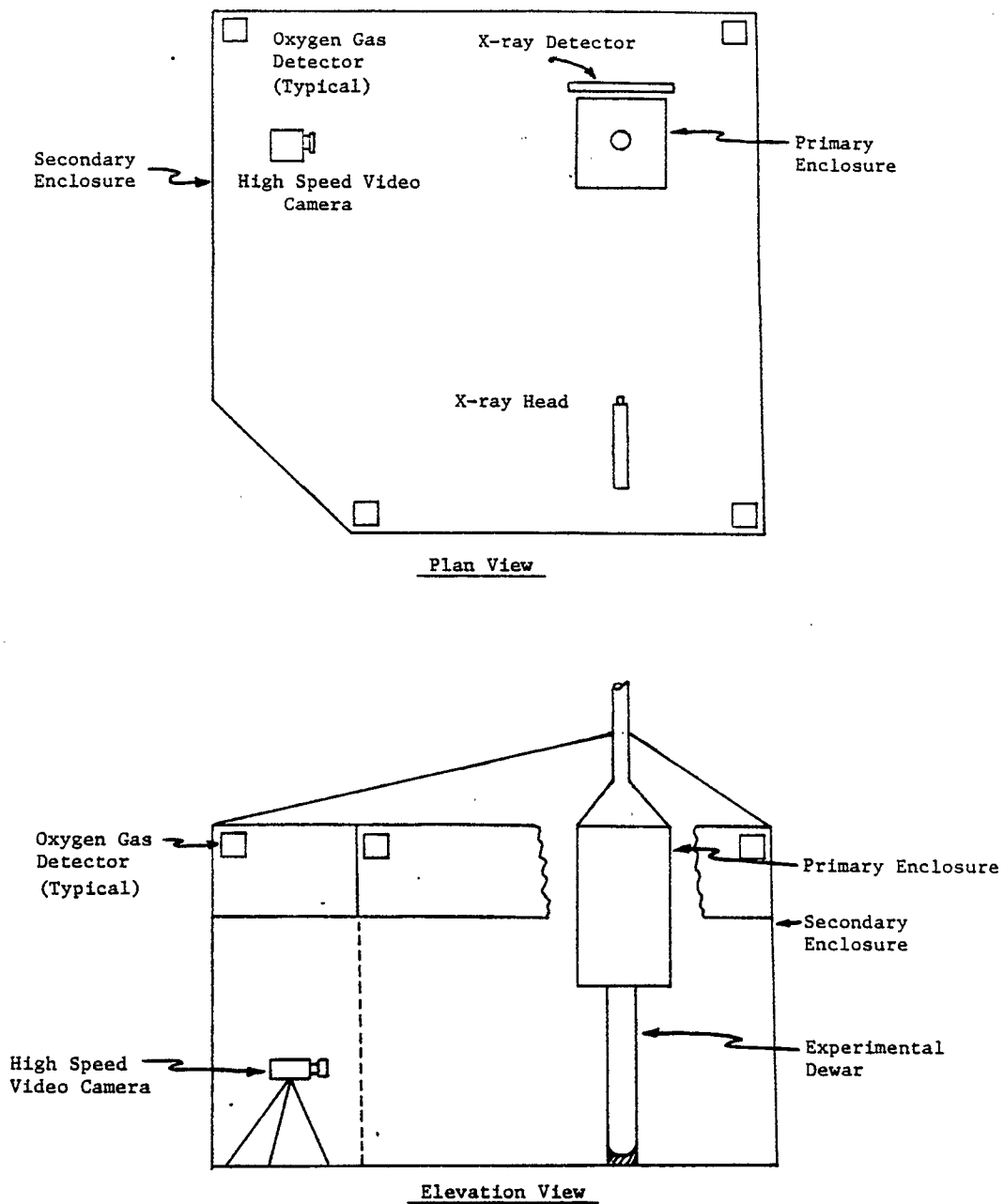


Figure 2. Facility schematic.

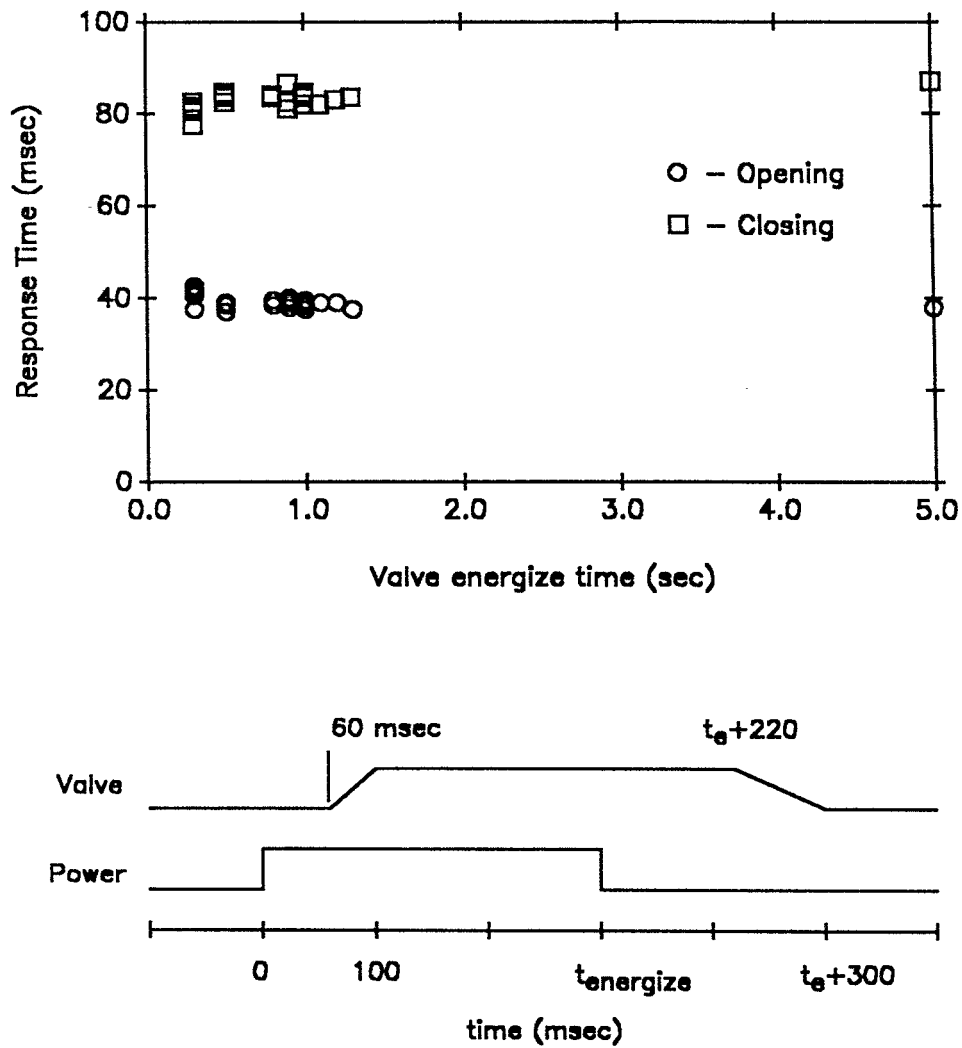


Figure 3. Dump valve response characteristics.

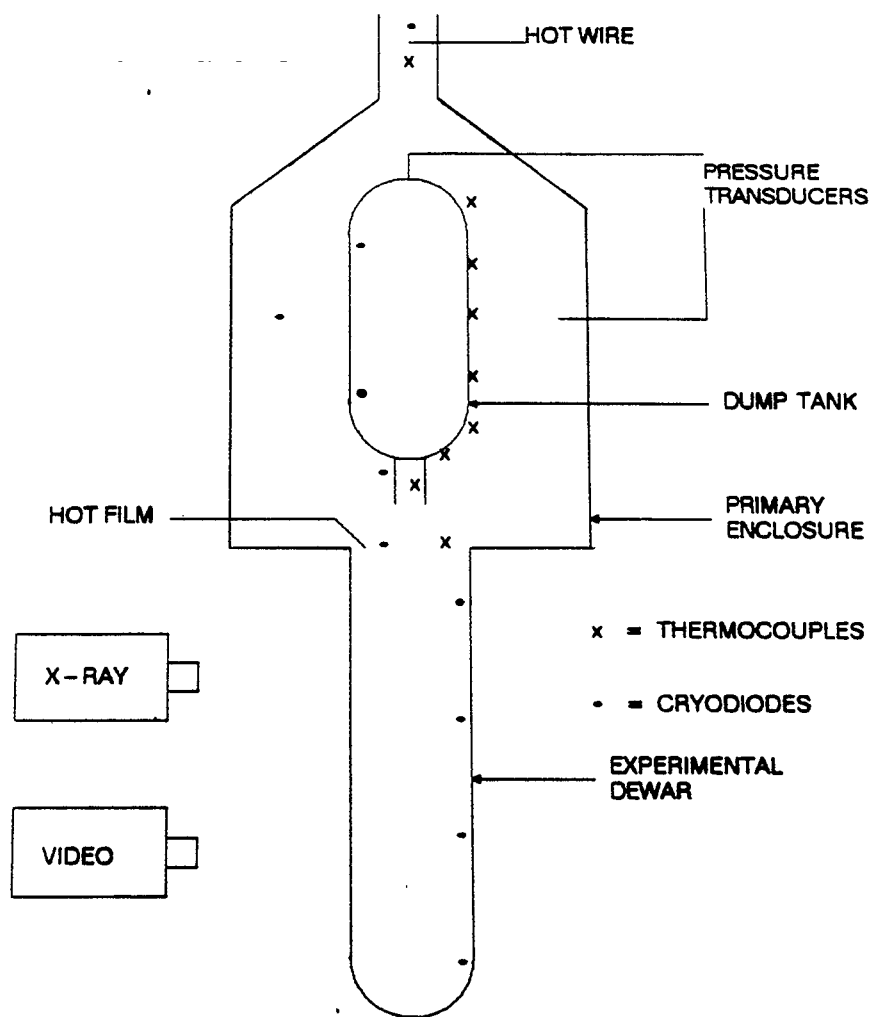


Figure 4. Schematic of primary enclosure.

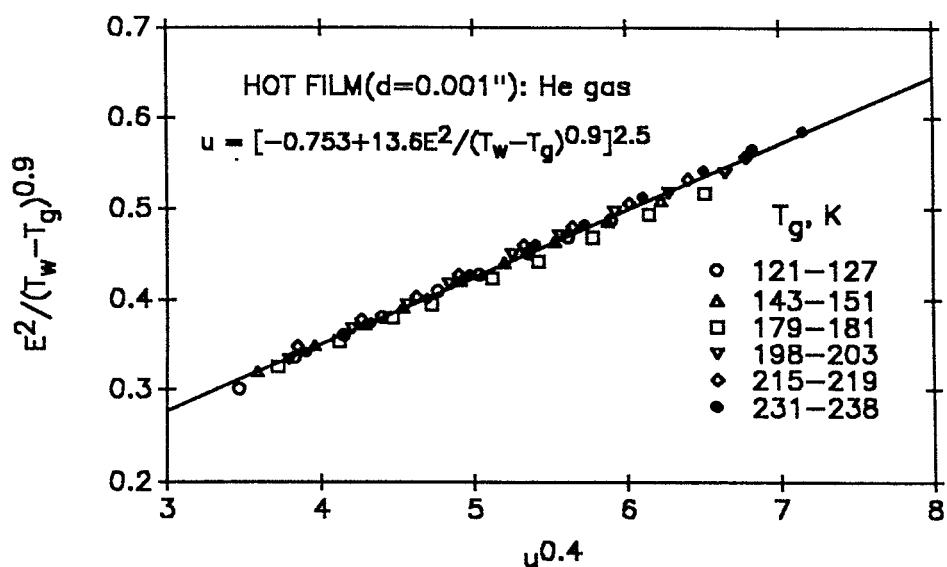


Figure 5. Hot-film anemometer calibration curve.

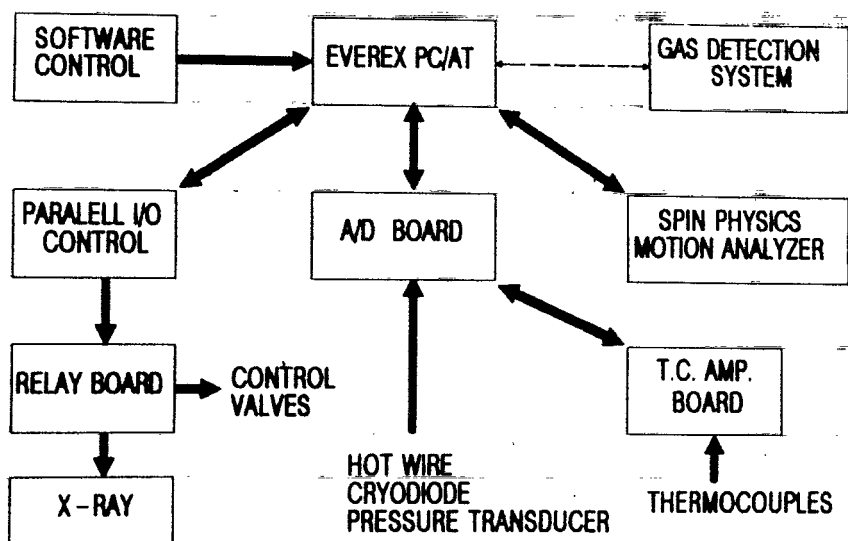


Figure 6. Data acquisition system

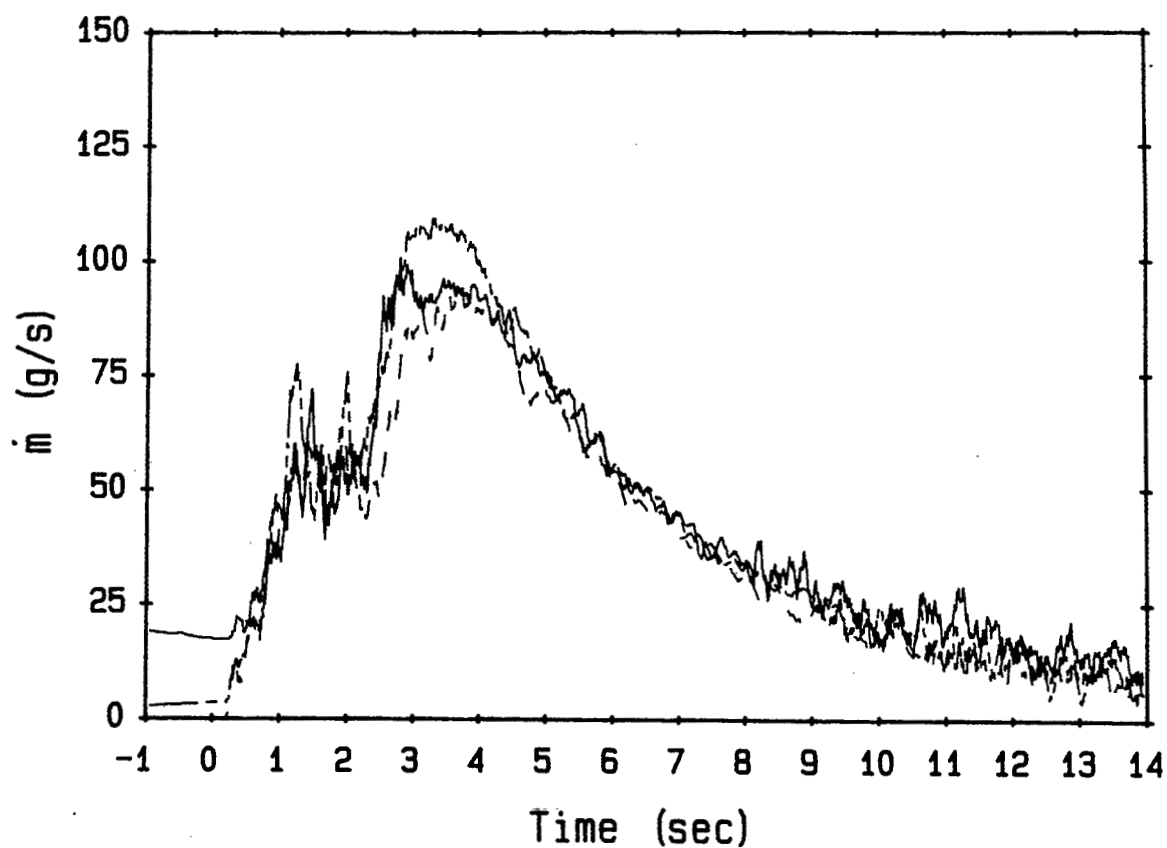


Figure 7. Helium evaporation rate for three similar tests.

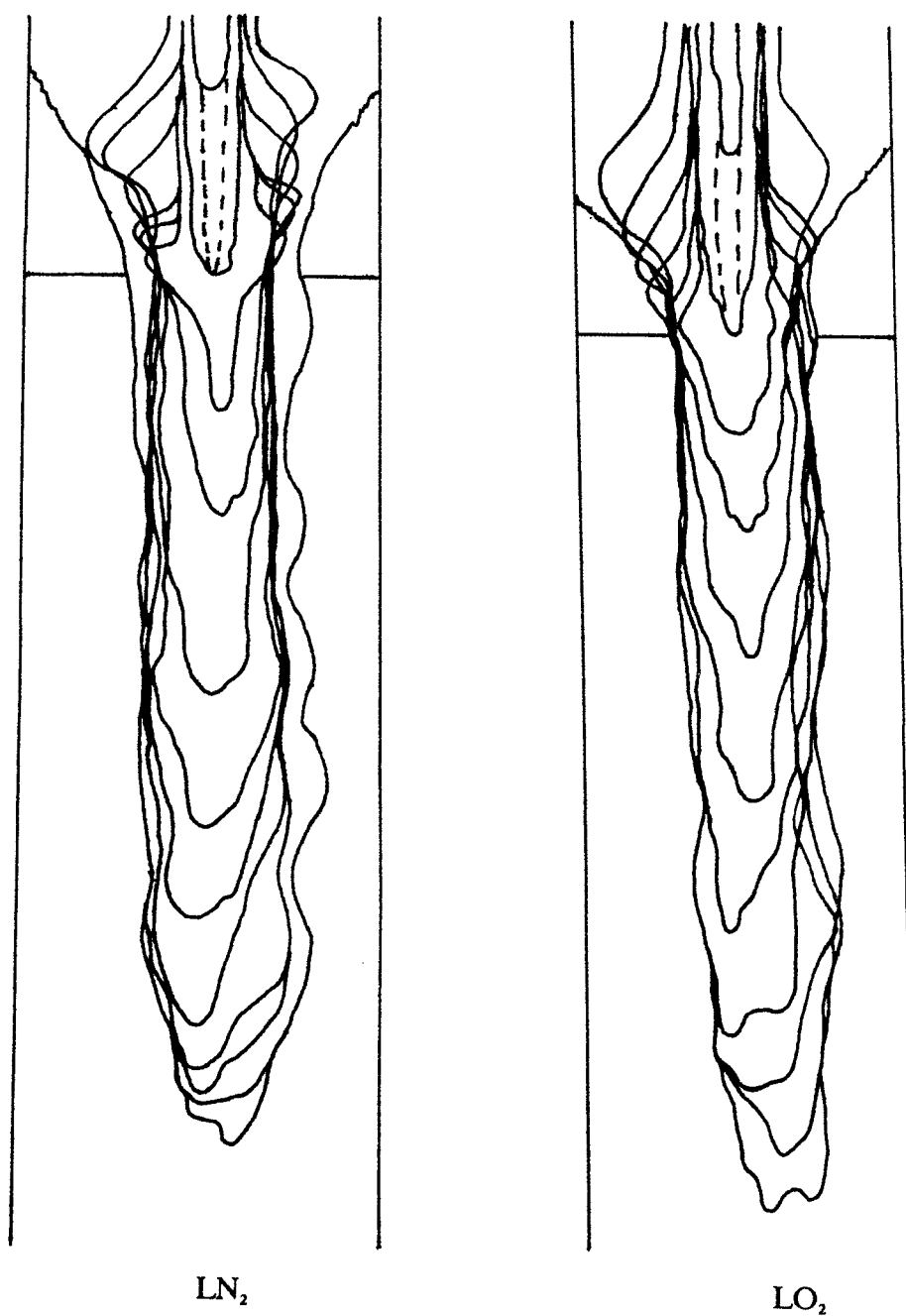


Figure 8. Mixing zone contours for LO_2 and LN_2 jets into LHe

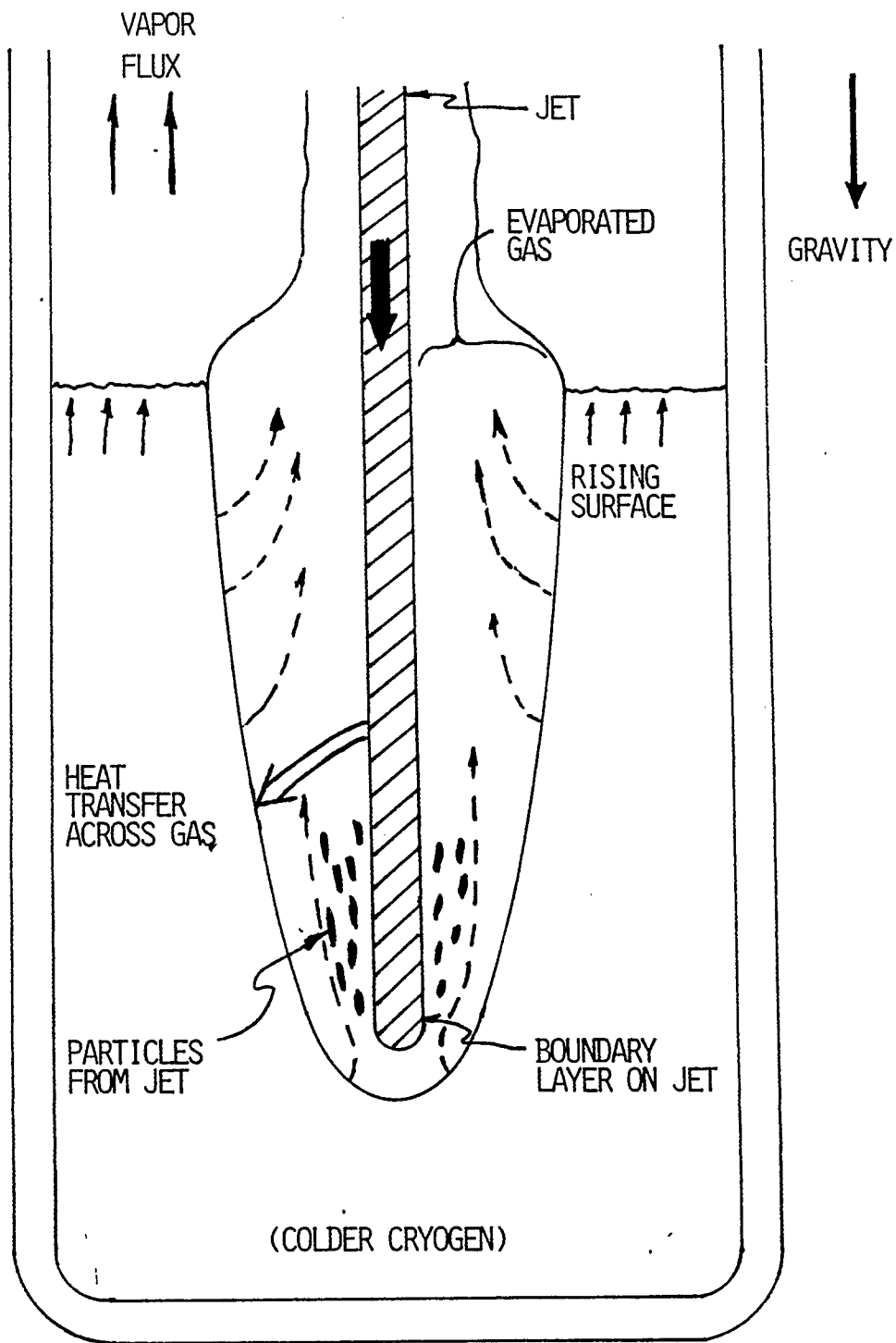


Figure 9. General mixing zone characteristics.